University of Kent

Kent Academic Repository

Martínez Jiménez, Alejandro, Hughes, Michael, Dorrington, Hal and Podoleanu, Adrian G.H. (2025) *Off-axis endoscope implementation for swept-source full-field optical coherence tomography*. In: Optical Coherence Tomography and Coherence Domain Optical Methods in Biomedicine XXIX (PC13305). . Society of Photo-Optical Instrumentation Engineers (SPIE)

Downloaded from
https://kar.kent.ac.uk/109792/ The University of Kent's Academic Repository KAR

The version of record is available from
https://doi.org/10.1117/12.3046461

This document version
Author's Accepted Manuscript

DOI for this version

Licence for this version
UNSPECIFIED

Additional information

Versions of research works

Versions of Record
If this version is the version of record, it is the same as the published version available on the publisher's web site. Cite as the published version.

Author Accepted Manuscripts
If this document is identified as the Author Accepted Manuscript it is the version after peer review but before type setting, copy editing or publisher branding. Cite as Surname, Initial. (Year) 'Title of article'. To be published in ***Title of Journal*** , Volume and issue numbers [peer-reviewed accepted version]. Available at: DOI or URL (Accessed: date).

Enquiries
If you have questions about this document contact ResearchSupport@kent.ac.uk. Please include the URL of the record in KAR. If you believe that your, or a third party's rights have been compromised through this document please see our Take Down policy (available from https://www.kent.ac.uk/guides/kar-the-kent-academic-repository#policies).

Off-axis endoscope implementation for swept source full field optical coherence tomography using a miniature camera

A. Martinez Jimenez*, M. Hughes, H. Dorrington, A. Podoleanu

Applied Optics Group, School of Physical Sciences, University of Kent, Canterbury CT2 7NH, United Kingdom
*E-mail: am2571@kent.ac.uk

1. Introduction

Recently, non-scanning modalities such as Full-Field Swept Source OCT (SS-FF-OCT) have gained interest due to the ability of imaging whole volumes in fractions of seconds with high-sensitivity and stable in phase. An inherent problem of FF implementations is given by the crosstalk from different pixels; however, improvements have been made by several methods [1]. Building on this success, new arrangements including endoscopes have emerged in different areas [2]. For most endoscope probes, highly technical engineering solutions are required, needing to assemble miniaturized probes, such as side viewing OCT systems via rotatory joints. In fact, most recent developments towards endoscopy OCT have been dominated by side-viewing probes. Although side viewing is of high interest for vascular or cylindrical shape inspection, many procedures such as laryngoscopy, bone inspection [3], will benefit from forward viewing imaging [4]. In this work, we present a novel alternative for miniaturization, based on forward viewing SS-FF-OCT and off-axis interferometry. To validate the potential of the model, we study its off-axis characteristics using a professional camera, with the intention to miniaturize the assembly in front of a much smaller camera at a later stage.

2. Methods

Fig. 1 shows a schematic set-up of the forward endoscope SS-FF-OCT. The light of a swept source is sent via a PM coupler to a reference and a sample arm. Here the fibers are cut at an angle that deviates light off-axis, in order to flood illuminate the object as well as flood illuminate the camera. Such configuration will allow miniaturization into a probe head of 2-3 mm diameter and of less than 2 cm, depending on the focal length of the lenses used. The axial resolution will be given by the tuning bandwidth of the swept source and the volume acquisition will be determined by the frame rate of the camera.

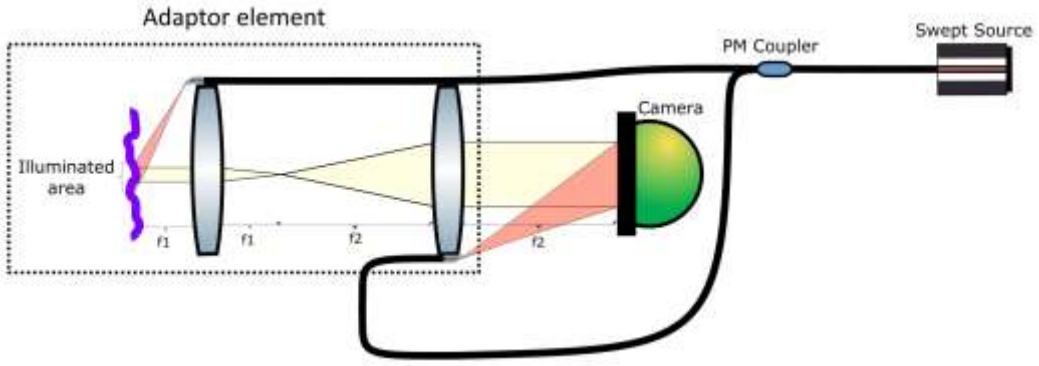


Figure 1 Schematic set-up off-axis interferometer adaptor.

In order to study the effects of the off-axis interferometry on a SS-FF-OCT as that in Fig. 1, a simpler and more amendable system is used in Fig. 2. The swept source (BS-790-1-OEM, Superlum) output light is linearly polarized, as such PM couplers are used to avoid polarization mode dispersion. A camera (EoSens 10CXP2, Mikrotron) acquires images at 1000 Hz with 12 bits and is triggered by the swept source. In Fig. 2(a), the light from the swept source is sent by a PM coupler into two arms. Here we define the sample arm, as the path at an angle β from the normal to the camera in the plane of the sketch, and the reference arm, the path along a perpendicular to the camera, both measured from the coupler, where the two fiber coupler leads are equal in length. The sample and reference arm are collimated via reflective mirror collimators obtaining beam diameters of 1.4 mm. In both arms, half waveplates (AHWP06M-980, Thorlabs) and linear polarizers (LPNIRB, Thorlabs) are placed. Combined with the linear polarization input light, these elements enable the change of the orientation of polarization direction by an angle α measured in relation to the sketch plane. On the following we study two alternatives for the poalrization orientation of the two waves in the two arms. At first when polarizations are oriented along the x direction, so $\alpha = 90^0$, i.e. perpendicular to the plane of the sketch, and secondly when $\alpha = 0^0$, i.e. in the plane of the sketch. The difference with Fig. 2 (b) resides on the addition of a lens of 5 cm focal length placed at 6 cm from the

camera. This lens generates a divergent beam towards the camera that combined with the reference arm, produces a nonlinear variation of the optical path along the angle.

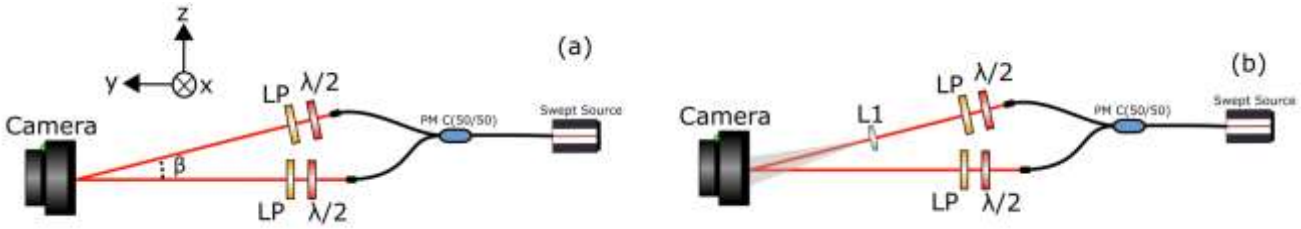


Figure 2 Set-up for (a) β angle variations and polarization variations; and (b) divergence examination.

3. Results

Figure 3(a) shows a B-Scan through the z plane. Consequently, the walk-off produced by the displacement of the coherence gate over the camera can be seen. Due to the angle between sample and reference arm, β, a larger walk-off can be observed for $\beta = 13.4^0, 18.9^0$ and 28.9^0 respectively in the three images in Fig. 3 (a). Those represent the variation in OPD with the angle β. As the tilt increases, the signal is also reduced when the light is sent into the camera with an angle. For instances, in Fig. 3(b) the three categories of spread points represent; the blue dots: the intensity in the camera only along β with $\alpha = 0$; Red and yellow dos respectively: the peak intensity of the FFT for variations along β, for $\alpha = 0$, and $\alpha = 90$. Using the setup in Fig. 2 (b) an *en-face* image is presented in Fig. 3(c). This shows that the contour is not along a straight line, due to the curvature of the wavefront in OPD along the camera pixels. In order to display the effect of using a divergent reference beam, two B-Scans at different positions in the camera, marked in yellow, are shown on right side of Fig. 3 (c).

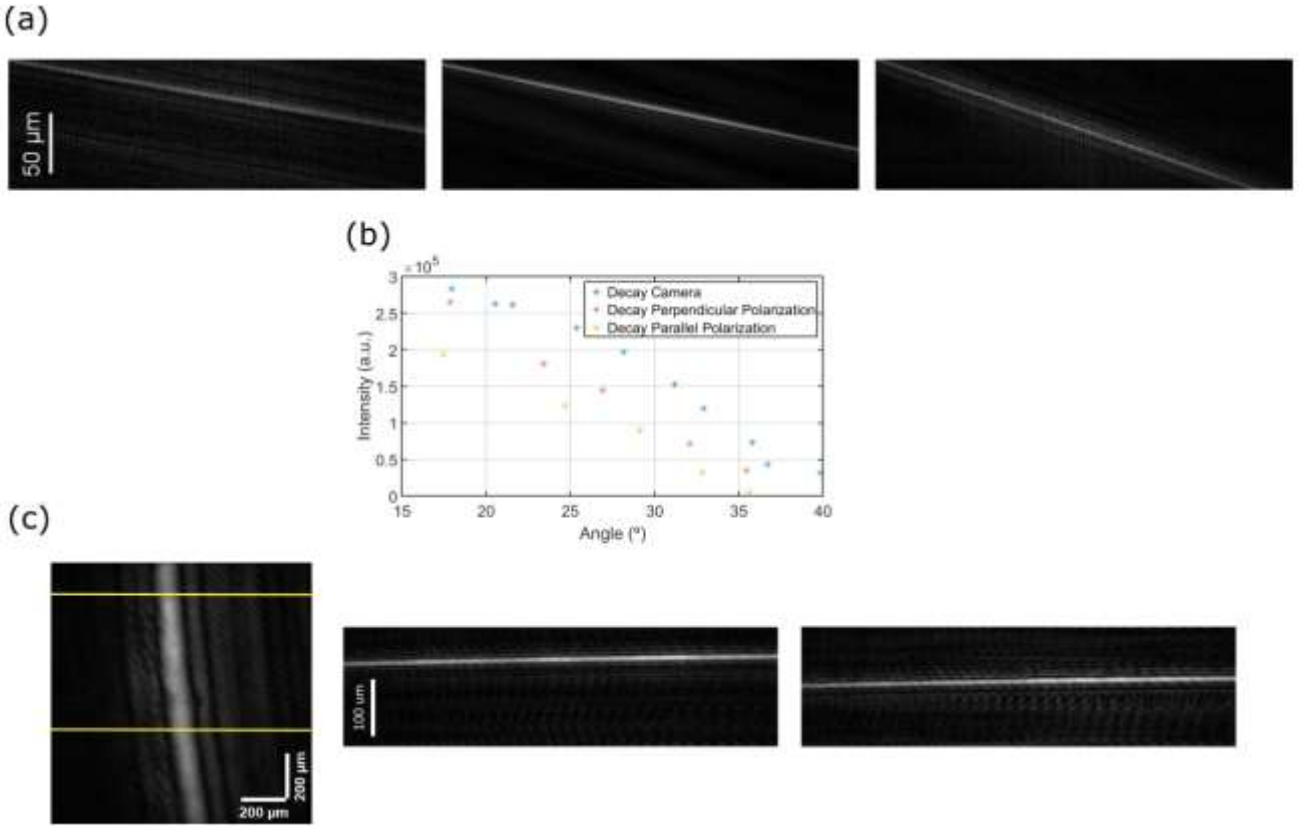


Figure 3 . (a) Tilt of the B-scan due to increase in the angle β. (b) Decay of interference measured at an OPD close to 0.1 mm versus angle β (c) *En-face* image obtained with a divergent beam lined in yellow with the positions of the B-Scans on the right, from top to bottom.

4. Discussion & conclusions

The proposed forward viewing model requires careful optimization of the free parameters such as the polarization state, the offset β angle, and the coupling ratio. In addition, there is variation of the OPD with inclination of the wavefront in Fig. 3 (a) as well as variation of OPD due to divergent illumionation in Fig. 2 (b). These variations can be explained by the divergent shape of the Gaussian beam travelling larger OPDs on the extremes. From Fig. 3(b) is important to notice that the intensity, and therefore the sensitivity might be affected for larger β values. Although this can be overcome by using larger powers, it might restrict the use for biological samples when power safety is a requirement. Here, as the swept source is linearly polarized, special attention needs to be made for the sample illumination. We observe a higher decay for values on $\alpha = 0$. Overall, it should be noticed that there are two decays when varying β for $\alpha = 0$, the intrinsic decay due to the projection of energy on the camera, and the decay due to the Malus law. An optimum design for the miniaturization of the adapter [6] should consider all these requirements. Further results using the optimal parameters and OCT images using the adaptor element will be presented in the conference.

References

[1] Egidijus Auksorius, Dawid Borycki, and Maciej Wojtkowski, "Multimode fiber enables control of spatial coherence in Fourier-domain full-field optical coherence tomography for in vivo corneal imaging," Opt. Lett. 46, 1413-1416 (2021)

[2] Michalina J. Gora, Melissa J. Suter, Guillermo J. Tearney, and Xingde Li, "Endoscopic optical coherence tomography: technologies and clinical applications [Invited]," Biomed. Opt. Express 8, 2405-2444 (2017)

[3] Evan T. Jelly, Zachary A. Steelman, and Adam Wax, "Optical coherence tomography through a rigid borescope applied to quantification of articular cartilage thickness in a porcine knee model," Opt. Lett. 44, 5590-5593 (2019)

[4] Wurster, L. M., Shah, R. N., Placzek, F., Kretschmer, S., Niederleithner, M., Ginner, L., ... & Ataman, Ç. (2019). Endoscopic optical coherence tomography angiography using a forward imaging piezo scanner probe. Journal of biophotonics, 12(4), e201800382.

[5] Ansari, Z., Gu, Y., Tziraki, M., Jones, R., French, P. M. W., Nolte, D. D., & Melloch, M. R. (2001). Elimination of beam walk-off in low-coherence off-axis photorefractive holography. Optics Letters, 26(6), 334-336.

[6] A Podoleanu, M Marques, M Hughes - US Patent 11,717,154, 2023